2021 European Conference on Computing in Construction
Ixia, Rhodes, Greece
July 25-27, 2021

COMPARISON OF ACCURACY AND DENSITY OF STATIC AND MOBILE LASER SCANNERS

Maciej Trzeciak[1], Ioannis Brilakis[1]
[1]Department of Engineering, University of Cambridge, United Kingdom

ABSTRACT

We test the accuracy and density of mobile lidar-based scanners and compare them with the performance of a static scanner. This is achieved by systematically scanning a rectangular target at a growing distance, collating the statistics of the scans and comparing them. This study shows that the accuracy of the scans outputted by the static scanner is about 20 times better at 5 meters than those produced by the mobile devices and this gap further increases along with the distance. The density, measured in points per second, drops along with the distance for all the tested devices, with mobile scanners outperforming their static counterparts.

INTRODUCTION

The construction industry is among the least digitised compared to all other industries worldwide. It is estimated that improving digitisation in this area could significantly boost productivity, potentially creating $1.6 trillion of added-value, which is equal to half of the world's infrastructure needs (McKinsey Global Institute, 2017).

One of the key components of digitisation is the ability to create accurate 3D scans of an environment using cameras or a lidar (Light Detection and Ranging) (Cadena et al., 2016). The ability to efficiently capture the geometry of built and under-construction assets is a fundamental step towards enabling the digitisation of the built environment.

Static laser scanners (e.g. FARO Focus 3D) and photogrammetric software (e.g. Bentley Context Capture) are well known in the construction industry. The last decade has brought a proliferation of mobile scanning solutions that can collect data quicker, thus leading to lower operational costs. They are relatively newer and the knowledge of their true performance is very limited. Lidar-based hand-held scanners seem the dominating solutions for outdoor mobile mapping (Lee et al., 2019) thanks to their reliability and scanning range – significantly higher than the range of stereoscopic depth cameras such as Intel RealSense (Keselman et al., 2017) or structured-light cameras such as Google Tango (Marder-Eppstein, 2016). Yet the available scanning solutions are rarely tested against a common benchmark to allow for comparisons.

Figure 1: Scanning a target using static (on the left) and mobile (in the middle) laser scanners.

In this paper, we measure the performance of 2 commercially available lidar-based mobile scanners and compare it to that of a static scanner. We do that by systematically scanning a rectangular target of known dimensions (Figure 1) at distances ranging from 5 to 40 meters with a 5-meter interval and collating the statistics of the obtained pointclouds. In particular, we focus on the accuracy/noise and the density as the former is crucial in the case of accurate engineering surveying (RICS, 2014) while the latter makes the scanned objects more informative to the user. We also compare the obtained results against the requirements of certain use cases in the Architecture, Engineering and Construction (AEC) industries, including engineering surveying – a use case chosen for this paper as one of the most frequent ones in the AEC industry (RICS, 2020). It should be noted, however, that the mobile scanners are not marketed to meet the RICS specification for engineering surveying, and we compare the performance of these devices against this use case solely to add a tangible reference point for professionals using such devices. We hope this paper will increase the awareness of how static and mobile scanning devices perform, and open up the door for further research and improvements in this area, especially in mobile mapping.

The next chapter describes in detail how to determine the accuracy of a pointcloud of a target , followed by the detailed description of our data collection process. We then present the qualitative and quantitative results of the accuracy and density analyses which are concluded with a discussion and implications to the industry.

METHODS

Determination of pointcloud noise

The UK's Royal Institution of Chartered Surveyors defines the accuracy as 2 standard deviations from the true value (equation 1) in the context of building and land surveying (RICS, 2014). A set $D = \{d_i\}$ denotes the distances of points from the ground truth. Such a definition can be seen as a noise measure. Therefore, the notions of accuracy and noise will be interchangeably used in this paper. Equation 1 corresponds to the probability that 95% of the points lie within the accuracy if set D follows a Gaussian distribution. Formula 1 is also in line with (Bergelt et al., 2017) although the authors equate noise to 1 standard deviation.

$$accuracy = 2\sigma = 2\sqrt{\mathbb{E}[D^2] - (\mathbb{E}[D])^2} \quad (1)$$

In this paper, we further split the noise into 2 components: the noise perpendicular to the fit plane (the depth/range noise) and the remaining part – the "vertical noise". Since the latter can be associated with the accuracy of the area of our rectangular target, we replace it with simply measuring the area of a rectangle that covers the pointcloud of the target. Another reason for this simplification is that the open-source software Cloud Compare cannot compute the noise defined as in equation 1 for a rectangular shape of known dimensions. We have decided to use Cloud Compare as it is very well known to the industry and its use makes the process described in this paper relatively smooth and easily reproducible.

The depth/range noise involves measuring distances from the true value of a planar target in our experiment. Accordingly, there must be a mean to fit a plane to the obtained pointcloud as shown in Figure 2. Such a fit plane will serve as the ground truth in our experiment and the distances $\{d_i\}$ can be computed as in formula 2.

$$d_i = \frac{|A(x_i - x_0) + B(y_i - y_0) + C(z_i - z_0)|}{\sqrt{A^2 + B^2 + C^2}} \quad (2)$$

Fitting a plane to a pointcloud defined this way is then a multivariate optimisation problem for which we will be using a feature in Cloud Compare which finds such a Euclidean transformation H of the plane that minimises the Root Mean Square (RMS) error of the distances D according to formula 3. The plane consists of a normal vector $(A, B, C)^T$ and a point belonging to the plane $(x_0, y_0, z_0)^T$.

$$H^* = \arg\min_H RMS(D) \quad (3)$$

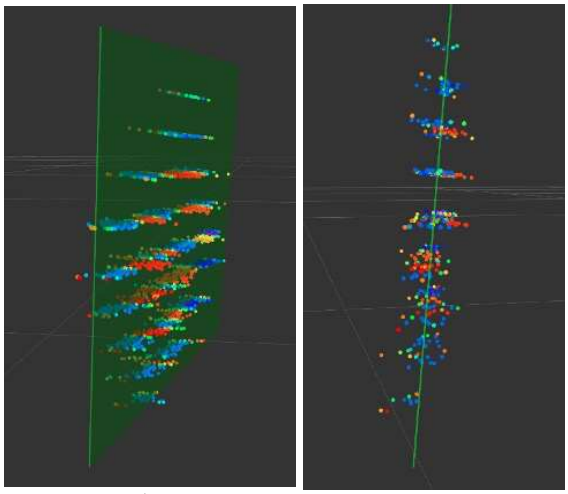

a) b)

Figure 2: Fitting a plane to an isolated pointcloud of a planar target: the general view (a) and the side view (b).

DATA COLLECTION

Scanners

In our experiment we use 1 static and 2 mobile laser scanners: (1) FARO Focus 3D; (2) GeoSLAM ZEB Horizon; (3) KAARTA Stencil 2 respectively. They are presented in Figure 3.

Both mobile scanners are equipped with a lidar sensor shooting 300,000 points per second of accuracy (1 sigma) ±30 mm and can produce scans at a 100-meter range according to their specifications (GeoSLAM, n.d.; Smith, n.d.). Their weight does not exceed 2.8 kg and they both have 360° horizontal Field of View (FoV). Vertical FoV is 270 degrees for the GeoSLAM's product and 30° for the KAARTA's. This difference is caused by the fact that the former has a mechanical system rotating the lidar, hence increasing its FoV. Another apparent difference is that the KAARTA's scanner does have an inherent grayscale camera in its basic version whereas the other scanner can be equipped with an RGB camera after an upgrade. The difference stems from the fact that the system of Stencil 2 uses the camera to improve the estimation of its trajectory (Shan and Englot, 2018) while ZEB Horizon uses imagery to colourise pointcloud.

On the other hand, FARO Focus 3D X 330 is equipped with a laser scanner of range 330 meters with an accuracy of 2 standard deviations at 25 meters equal to 1 mm in case of 10% reflective surface (FARO, 2016). Its vertical and horizontal FoVs are 300° and 360° respectively, with the step size of 0.009° in both directions. We set 'point distance' to be 6.136 mm/10m and 'scan size' to 10240x4267 points which corresponds to predefined indoor scanning settings for distances above 10 meters. The predicted scanning duration is around 8 minutes for such a setup. The resolution and quality could be further improved at the cost of increased time.

a) b) c)

Figure 3: We use a static laser scanner FARO Focus 3D (a) and two mobile laser scanners – GeoSLAM ZEB Horizon (b) and KAARTA Stencil 2 (c).

Scanning a target

The same wooden rectangular target of size A1 sheet of paper (0.841m x 0.594m = 0.500m^2) is scanned indoors at distances ranging from 5 to 40 meters with a 5-meter interval as shown in the first row in Figure 4. As indicated in (Huang and Grizzle, 2020), placing the target so that its top and bottom edges run parallel to the lidar's rings lead to ambiguity in the vertical position of the target caused by the increasing spacing of the rings along with the distance. Therefore, the target is slightly rotated.

The scans of the target are systematically taken using the 3 scanners one after another for the same distance. The target is then moved by 5 meters forward and the 3 subsequent scans are taken again. We repeat this process until the last target is captured at a distance of 40 meters.

We stand still in the same place indoors during scanning the target using mobile devices and move them using a hand to simulate the real data collection process. We move the mobile devices around the lemniscate (a shape resembling the infinity symbol) in the planes both parallel to the target as well as perpendicular to it for around 10 seconds for each scan. Also, the performance of scanning devices depends on the environment (Shan and Englot, 2018; Zhang and Singh, 2014). Therefore, scanning from the same spot indoors unifies the environmental conditions and scene attributes so that their impact is the same for all the tested devices.

It is also worth noting that the KAARTA scanner needs to be constantly in the move to cover the whole target reasonably densely. This is especially true when the distance to the target increases and fewer and fewer lidar's beams cover the target.

Processing

After scanning, the collected data is transferred to a PC using an SD-card and a USB-stick for the static and mobile scanners accordingly. Each of the devices has its proprietary system in which the raw data is processed. We use the FARO SCENE 7.1 for the FARO scanner and the GeoSLAM Hub v5 for the ZEB Horizon. The Stencil 2 has its program installed on Ubuntu Linux directly on the device and the user can operate it via a tablet. While the first two software products needed around 30-60 seconds to process each of the scans, the KAARTA's software outputted a pointcloud right after scanning.

The processing is done with mostly default software configuration, turning off any additional sharpening and filtering where possible. The format for the outputted scans is .e57 in the case of FARO and .ply for the remaining two devices.

Post-processing

Finally, all the obtained scans are edited in Cloud Compare so that only the points belonging to the target are left. The isolated targets in the form of pointclouds can be seen in the last 3 rows in Figure 4. The number of points belonging to the target is divided by the time the scanning process takes. The output is then the number of points per second. We next fit a plane to each pointcloud of the target coming from each scanner and each distance separately and measure the smallest rectangle that covers the whole scan. Moreover, the depth noise is read off as an RMS parameter after fitting the plane. The reader might notice that RMS and standard deviation from formula 1 are the same, assuming that the mean is equal to 0 and both formulas divide the sum of squares by the number of addition components. Hence, no need for further computation of depth noise.

RESULTS

Qualitative results in the form of isolated pointclouds of the target at different distances from the 3 scanners are presented in Figure 4. The first row contains the photos of the targets at different distances. Isolated scans of the target coming from the FARO scanner are in the second row, followed by the scans from the KAARTA device in the third row and from the GeoSLAM scanner in the last row. There are also rectangles surrounding the pointclouds in the last two rows to better visualise the increasing vertical noise of the scans produced by the mobile devices. The scale across all the presented scans is preserved so the reader can have an even better notion of the problem.

The quantitative results corresponding to the qualitative results from Figure 4 can be seen in Figures 5, 6 and 7. Figure 5 presents the number of points belonging to the target divided by the time the scanning took. It was about 8 minutes in the case of the static scanner and around 10 seconds for both mobile devices.

Figure 6 and 7 correspond to the noise levels – the former presents the depth/range noise after fitting a plane to the scans of the target while the latter represents the area of the minimal rectangle covering the pointclouds which, in turn, refers to the rectangles surrounding the pointclouds of the target in the last 2 rows of Figure 4.

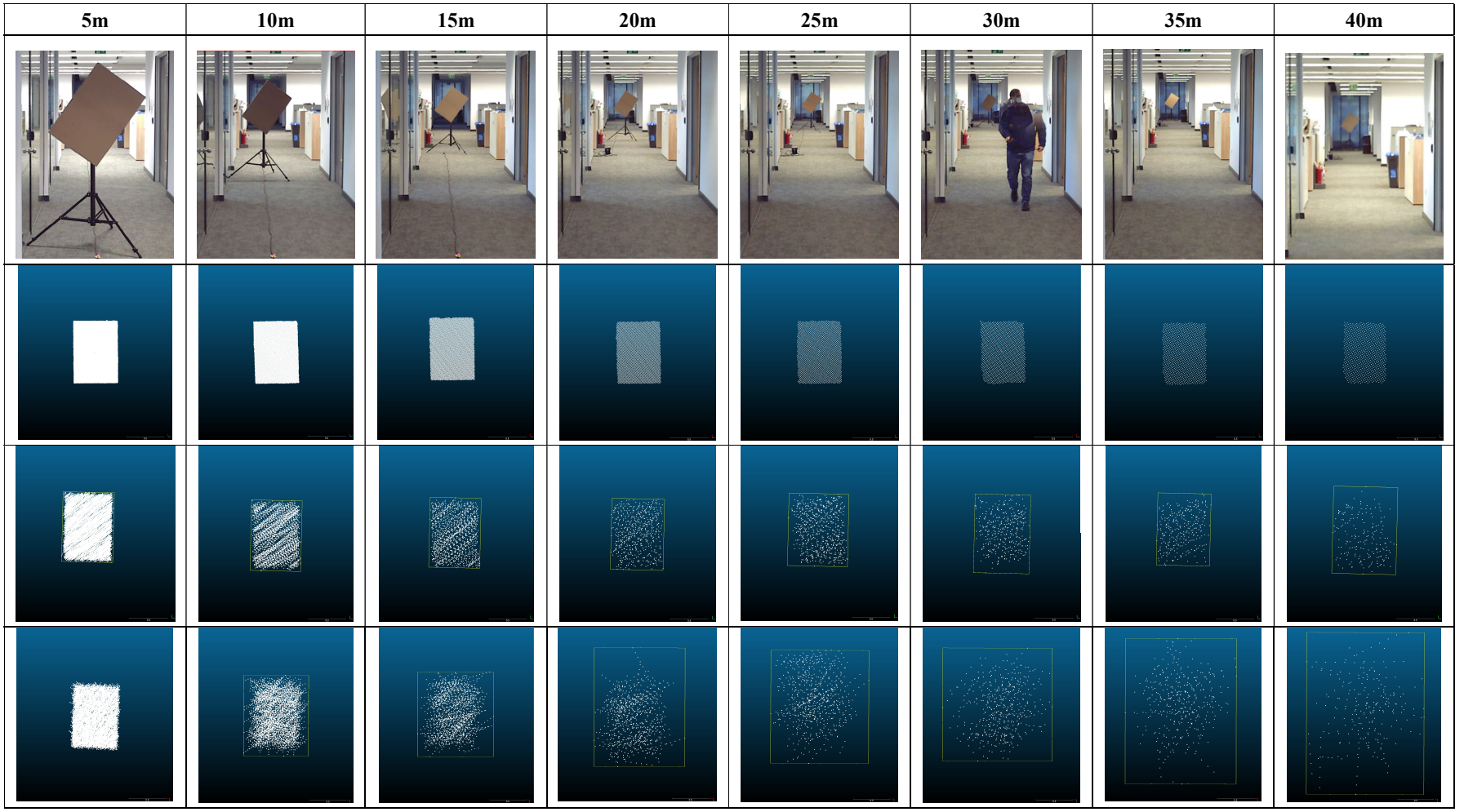

Figure 4: A rectangular target scanned by 3 different scanners at distances 5-40 meters: 1st row – view of the target from a camera, 2nd row - target by the FARO static laser scanner, 3rd row – target by the KAARTA Stencil 2, 4th row – target by GeoSLAM ZEB Horizon.

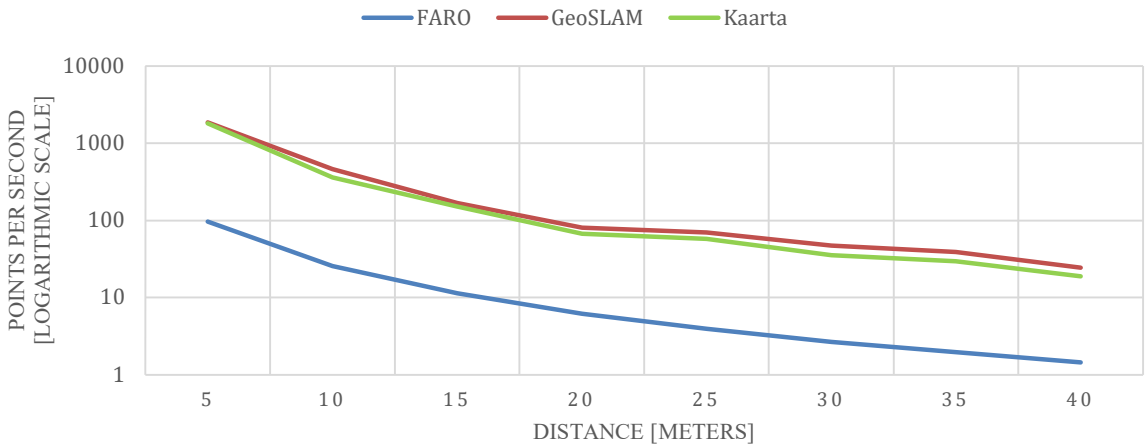

Figure 5: Number of points belonging to the target per second.

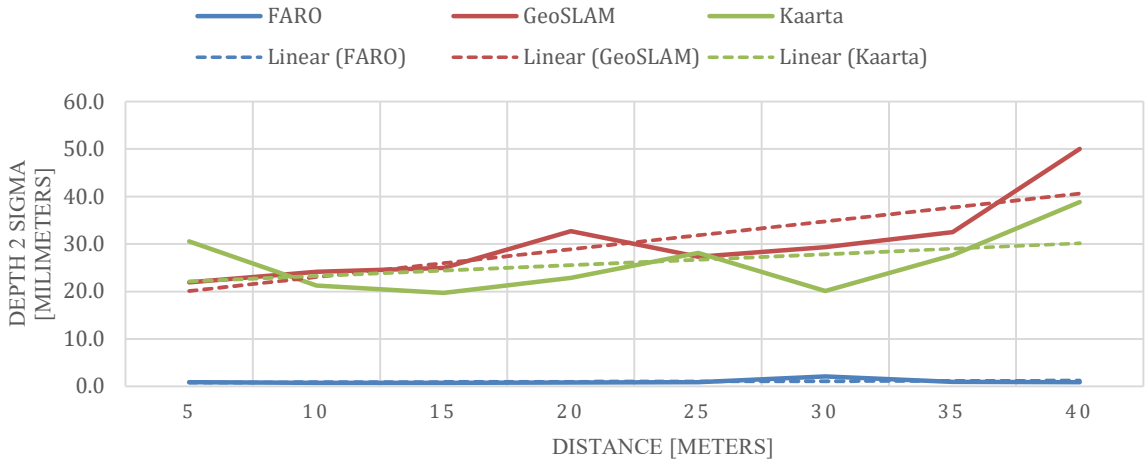

Figure 8: Depth accuracy of the scans of the target.

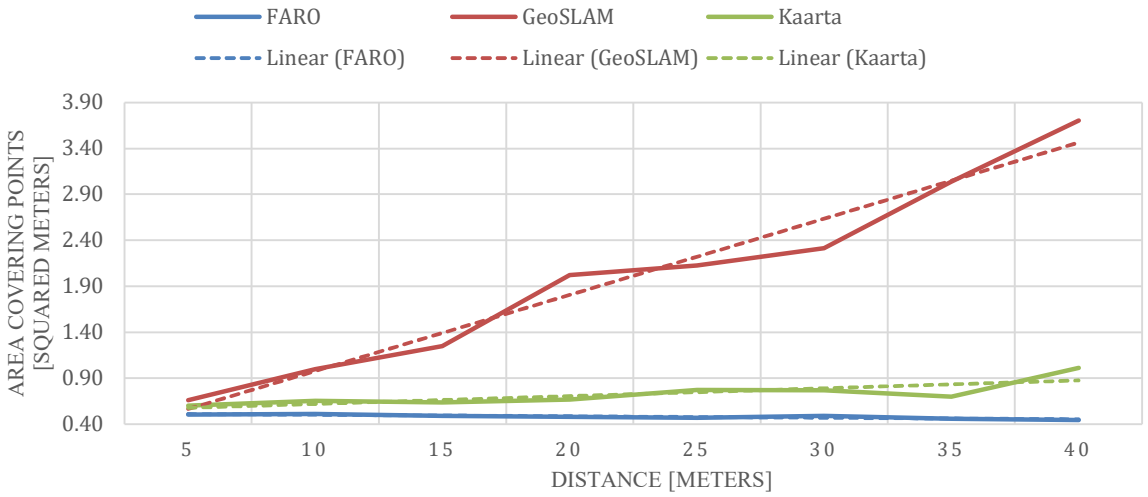

Figure 7:Area of the smallest rectangle covering the scans of the target.

DISCUSSION

There is a very apparent difference in density per second between the static and mobile scanners (Figure 5). The latter outperforms the former in the number of points produced on the target per second. This, however, dilutes along with the distance. The figure shows that initially a significant gap of around 1800 points per seconds at 5 meters, decreases exponentially to around 50-60 points at 20-25 meters, ending up at roughly 20 points per second at the distance of 40 meters. The relatively low density of the static scanner can be contributed to the fact that the head of the device rotates at 360° and maps everything around whereas we only take the number of points belonging to the target standing in front and divide that number by the time the full scan takes (which is about 8 minutes along with colouring the pointcloud). It is also worth noting that it takes a fixed amount of time for the static scanner to finish scanning for a given set of parameters while the number of points collected using the mobile scanners increases with time.

The depth/range noise of the scans measures the noise only along an axis perpendicular to the target. It remains steady for the static scanner at the level of around 1 mm while for mobile scanners it is 20-30 times higher at 5 meters and it gradually increases to reach about 40-50 times that value at 40 meters. It is also worth noting that this quantity alone (without the other part of the noise measured along the remaining two axes) meets the requirements of use cases such as (but not limited to) measured building surveys, topographic surveys and low accuracy setting out since it is lower than ±50mm at 5 – 35 meters for all the tested devices. However, the value in question is higher than ±20 mm at all the distances for both of the mobile scanners which is too high for meeting the specifications of engineering surveying as described in (RICS, 2014).

The remaining part of the noise – the vertical noise – is proposed to be measured in the plane of the target as the rectangle surrounding the pointcloud of the target (Figure 7). The rectangles around the scans by the static scanner are the closest to the correct dimensions of the target, followed by Stencil 2 and then ZEB Horizon. The areas of rectangles by KAARTA and GeoSLAM differ from those by FARO by 20% and 32% at 5 meters respectively and this deviation increases almost linearly across the whole range to 102% and 640% at 40 meters accordingly.

The gradual reduction of density and accuracy along with the distance to the target is a major impediment in the ability of detection tools to find edges and corners in scans. Our experiment shows that edges and corners become less and less recognisable as the distance increases. This might force the user working on such scans to guess their exact position, and consequently, decreases the correctness of engineering measurements on such scans.

There are also other points of interest – for example, whether or not the produced pointclouds contain colour information which could help the user to identify and recognise scanned objects easier (Cipolla, 2018). In our experiment, only the FARO scanner could output a pointcloud with RGB data, however, the respective upgrades for the mobile scanners are available.

Finally, the type of environment has an influence on mobile scanning. We tested all the devices under the same environmental conditions and scene attributes indoors to minimise this impact. Therefore, we isolated for whatever influence they might have on the results. However, real scenes in practice often contain moving objects such as vehicles and/or people. They are likely to increase the noise of the produced scans and partially distort them. Our experiment was carried out in a purely static environment.

CONCLUSIONS

In this paper, we present a simple though effective process of measuring the accuracy and density at a growing distance for static and mobile scanners. A rectangular target of known dimensions was systematically scanned by all the mapping devices at varying distances and its pointclouds were processed to collate their statistics. Our experiment showed that the density of the scanned targets measured in points per second decreases exponentially along with the growing distance to the target and that the mobile scanners outperform the static mapping devices in this regard. The trend is the opposite when it comes to accuracy. The static scanner produces scans that are at least 20 times less noisy than those by mobile devices. While the accuracy specifications for such use cases as measured building surveys, topographic surveys and low accuracy setting out are met by all the devices almost at the whole range up to 40 meters, the more demanding use cases such as engineering surveying could only be satisfied by the static scanner. We also conclude that the combined fact that the density and accuracy decrease along with the distance to the target, heightens the problems in finding edges and corners in scans forcing the user to guess their exact position. Also, the reader should look rather at trends in the outcomes presented in this paper and not exact values as the latter can change depending on the environment in which the scans are taken. Finally, this paper investigates measuring accuracy using a target of known dimensions at a growing distance which is one of many approaches to the accuracy measure. Our way, although relatively simple, seems to be quite challenging, particularly for mobile mapping devices.

ACKNOWLEDGMENTS

The research leading to this paper received funding from BP, GeoSLAM, Laing O'Rourke, Topcon and Trimble. The authors would like to thank these companies for making this research possible. We gratefully acknowledge the collaboration of all the industrial partners. Any opinions, findings, conclusions or recommendations expressed in this material are those of the authors and do not necessarily reflect the views of the entities mentioned above.

REFERENCES

Bergelt, R., Khan, O., Hardt, W., 2017. Improving the intrinsic calibration of a Velodyne LiDAR sensor. 2017 IEEE Sens. https://doi.org/10.1109/ICSENS.2017.8234357

Cadena, C., Carlone, L., Carrillo, H., Latif, Y., Scaramuzza, D., Neira, J., Reid, I., Leonard, J.J., 2016. Past, Present, and Future of Simultaneous Localization And Mapping: Towards the Robust-Perception Age. IEEE Trans. Robot. 32, 1309–1332. https://doi.org/10.1109/TRO.2016.2624754

Cipolla, R., 2018. Computer Vision, Handout 4: Stereo and Multiview Geometry.

FARO, 2016. Technical Specification Sheet for the Focus3D X 30/130/330 and X 130/330 HDR [WWW Document]. FARO® Knowl. Base. URL https://knowledge.faro.com/Hardware/3D_Scanners/Focus/Technical_Specification_Sheet_for_the_Focus3D_X_30-130-330_and_X_130-330_HDR (accessed 1.19.21).

GeoSLAM, n.d. GeoSLAM ZEB Horzion product specification [WWW Document]. GeoSLAM. URL https://geoslam.com/solutions/zeb-horizon/ (accessed 1.19.21).

Huang, J.-K., Grizzle, J.W., 2020. Improvements to Target-Based 3D LiDAR to Camera Calibration. IEEE Access 8, 134101–134110. https://doi.org/10.1109/ACCESS.2020.3010734

Keselman, L., Woodfill, J.I., Grunnet-Jepsen, A., Bhowmik, A., 2017. Intel RealSense Stereoscopic Depth Cameras. ArXiv170505548 Cs.

Lee, B.-U., Jeon, H.-G., Im, S., Kweon, I.S., 2019. Depth Completion with Deep Geometry and Context Guidance, in: 2019 International Conference on Robotics and Automation (ICRA). Presented at the 2019 International Conference on Robotics and Automation (ICRA), pp. 3281–3287. https://doi.org/10.1109/ICRA.2019.8794161

Marder-Eppstein, E., 2016. Project Tango, in: ACM SIGGRAPH 2016 Real-Time Live!, SIGGRAPH '16. Association for Computing Machinery, New York, NY, USA, p. 25. https://doi.org/10.1145/2933540.2933550

McKinsey Global Institute, 2017. Reinventing construction: A route to higher productivity.

RICS, 2020. Measured survey [WWW Document]. Glossary. URL (accessed 8.12.20).

RICS, 2014. Measured surveys of land, buildings and utilities. RICS guidance note, global. 3rd edition.

Shan, T., Englot, B., 2018. LeGO-LOAM: Lightweight and Ground-Optimized Lidar Odometry and Mapping on Variable Terrain. 2018 IEEERSJ Int. Conf. Intell. Robots Syst. IROS. https://doi.org/10.1109/IROS.2018.8594299

Smith, S., n.d. Stencil 2 for Rapid, Long-Range Mobile Mapping. KAARTA. URL https://www.kaarta.com/products/stencil-2-for-rapid-long-range-mobile-mapping/ (accessed 1.19.21).

Zhang, J., Singh, S., 2014. LOAM: Lidar Odometry and Mapping in Real-time, in: Robotics: Science and Systems. https://doi.org/10.15607/RSS.2014.X.007